13242–13253 *Nucleic Acids Research, 2014, Vol. 42, No. 21* *Published online 11 November 2014*
doi: 10.1093/nar/gku1150

Transcription bypass of DNA lesions enhances cell survival but attenuates transcription coupled DNA repair

Wentao Li, Kathiresan Selvam, Tengyu Ko and Shisheng Li*

Department of Comparative Biomedical Sciences, School of Veterinary Medicine, Louisiana State University, Baton Rouge, LA 70803, USA

Received July 04, 2014; Revised October 14, 2014; Accepted October 28, 2014

ABSTRACT

Transcription-coupled DNA repair (TCR) is a subpathway of nucleotide excision repair (NER) dedicated to rapid removal of DNA lesions in the transcribed strand of actively transcribed genes. The precise nature of the TCR signal and how the repair machinery gains access to lesions imbedded in stalled RNA polymerase II (RNAP II) complexes in eukaryotic cells are still enigmatic. RNAP II has an intrinsic capacity for transcription bypass of DNA lesions by incorporation or misincorporation of nucleotides across the lesions. It has been suggested that transcription bypass of lesions, which exposes the lesions, may be required for TCR. Here, we show that E1103G mutation of Rpb1, the largest subunit of RNAP II, which promotes transcription bypass of UV-induced cyclobutane pyrimidine dimers (CPDs), increases survival of UV irradiated yeast cells but attenuates TCR. The increased cell survival is independent of any NER subpathways. In contrast, G730D mutation of Rpb1, which impairs transcription bypass of CPDs, enhances TCR. Our results suggest that transcription bypass of lesions attenuates TCR but enhances cell tolerance to DNA lesions. Efficient stalling of RNAP II is essential for efficient TCR.

INTRODUCTION

Nucleotide excision repair (NER) is a multi-step process that removes bulky and/or helix-distorting lesions, such as ultraviolet (UV)-induced cis-syn cyclobutane pyrimidine dimers (CPDs) and bulky chemical adducts that generally obstruct DNA replication and transcription (1,2). NER has two subpathways: transcription coupled repair (TCR) and global genomic repair (GGR). TCR is dedicated to rapid removal of lesions in the transcribed strand of actively transcribed genes. On the other hand, GGR is responsible for removal of lesions throughout the whole genome, including the non-transcribed strand of actively transcribed genes. In eukaryotic cells, the two NER subpathways rely on different proteins in the early damage recognition step but share common factors in the later steps of the repair process. CSA, CSB, UVSSA and USP7 in mammalian cells (3,4) and Rad26 (homolog of mammalian CSB) in *Saccharomyces cerevisiae* (2) are involved in TCR but dispensable for GGR. On the other hand, XPC in mammalian cells (1), and Rad7, Rad16 and Elc1 in *S. cerevisiae* (2) are specifically required for GGR but play no role in TCR.

RNA polymerase (RNAP) is an ideal proxy damage sensor because its selectivity is higher than any known DNA damage recognition proteins (5). A mammalian RNAP II complex stalled at a CPD has a half-life of ∼20 h, which is more stable than any complex formed between a damage-recognition protein and its substrate (6). TCR is generally assumed to be triggered by stalling of an RNAP at a lesion in the transcribed strand, as DNA lesions that can substantially stall RNAP are generally good substrates for TCR (7,8). Up to date, however, no direct evidence has been available to prove this assumption and the precise nature of the TCR signal is still enigmatic.

In *Escherichia coli*, Mfd, a DNA translocase, binds to the β subunit of a lesion-stalled RNAP, displaces the RNAP complex by pushing it forward and concurrently recruits UvrA to the exposed lesion site to facilitate TCR (9–12). Upon binding to ATP, Mfd also binds to DNA in a manner that the DNA wraps around the protein (13). The DNA binding activity may anchor Mfd downstream from the transcription stop site to carry out its transcription-repair coupling function (14). In addition to promoting repair of lesions that stall the RNAP, Mfd may facilitate TCR downstream of the site that stalls RNAP (15). UvrD, a DNA helicase, has also been shown to play an important role in TCR in *E. coli* (16). Unlike Mfd, UvrD forces RNAP to backtrack, thereby exposing DNA lesions for access of the repair machinery.

How the TCR machinery gains access to a lesion initially trapped by a stalled RNAP II in eukaryotic cells is

*To whom correspondence should be addressed. Tel: +1 225 578 9102; Fax: +1 225 578 9895; Email: shli@lsu.edu

© The Author(s) 2014. Published by Oxford University Press on behalf of Nucleic Acids Research.
This is an Open Access article distributed under the terms of the Creative Commons Attribution License (http://creativecommons.org/licenses/by-nc/4.0/), which permits non-commercial re-use, distribution, and reproduction in any medium, provided the original work is properly cited. For commercial re-use, please contact journals.permissions@oup.com

still mysterious (7,8). Multiple scenarios have been suggested, including (i) ubiquitination and degradation of the largest subunit (Rpb1) of the 12 subunit (Rpb1–12) RNAP II, (ii) displacement of the transcription elongation complex through forced back- or forward-tracking and (iii) remodeling of the complex without removal from the arrest site. To date, however, none of these scenarios has been proven to be required for TCR in eukaryotic cells. In mammalian cells, CSB interacts loosely with the elongating RNAP II and stimulates transcription (17) but becomes more tightly bound following transcription arrest (18). CSB may also push the RNAP II forward, such that an additional nucleotide is incorporated opposite a CPD (19). However, unlike the bacterial Mfd, which displaces a lesion-stalled RNAP from the DNA, CSB does not seem to displace a lesion-stalled RNAP II (19). In *S. cerevisiae*, the elongating RNAP II complex, which is stabilized by Spt5 and other associated transcription elongation factors, is intrinsically repressive to TCR (20). Rad26 appears to facilitate TCR by antagonizing the repression, as it becomes dispensable for TCR in the absence of Spt4 (21,22), Rpb4 (23), the RNAP II associated factor 1 complex (PAFc) (24) and certain domains of Spt5 (20,21).

An RNAP has an intrinsic capacity for transcription bypass of lesions by incorporation or misincorporation of nucleotides across the lesions (25,26). *In vitro* studies with a DNA template containing a T-T CPD showed that the *S. cerevisiae* RNAP II catalyzes a non-templated insertion of AMP opposite the CPD 3′-T following the A-rule, followed by a very slow and templated AMP or UMP incorporation opposite the CPD 5′-T (27,28). AMP incorporation opposite the CPD 5′-T enables lesion bypass, whereas UMP misincorporation opposite the 5′-T results in irreversible stalling of RNAP II (27,28).

Two domains of Rpb1, the trigger loop and bridge helix, play key roles in the nucleotide addition cycle during RNA synthesis. Upon binding of a matched nucleotide, the trigger loop of RNAP II switches from an inactive open state to an active closed state (Figure 1) (29,30). Mutations of Rpb1 near the RNAP II active center and secondary pore (through which nucleotides reach the catalytic center) have been shown to affect the fidelity of transcription in *S. cerevisiae* (31–34). Two yeast Rpb1 mutations, G730D (*rpb1G730D*) and E1103G (*rpb1E1103G*) (Figure 1), have been shown to affect transcription bypass of CPDs *in vitro* (28). The *rpb1G730D* mutation is located in the α21 helix, which forms a part of the secondary pore and contacts the trigger loop. This mutation abolishes transcription bypass of a T-T CPD by preventing incorporation of nucleotides opposite the CPD 3′- and 5′-Ts. The *rpb1E1103G* mutation is located at the base of the trigger loop. In contrast to the *rpb1G730D* mutation, the *rpb1E1103G* mutation increases transcription bypass of T-T CPDs by enabling incorporation of two AMPs opposite the CPD 3′- and 5′-Ts (28). The *rpb1E1103G* mutation was also observed to increase resistance of *RAD26* (wild-type) cells but not *rad26Δ* cells to UV irradiation, suggesting that the increased UV resistance is dependent on Rad26-dependent TCR (28). An appealing new model of TCR mechanism was therefore proposed: transcription bypass of lesions may expose the lesions to the TCR proteins after their Rad26-dependent recruitment to the lesion-stalled RNAP II and this exposure may be required for TCR (28,35). However, if and/or how transcription bypass of lesions is implicated in TCR remains to be determined.

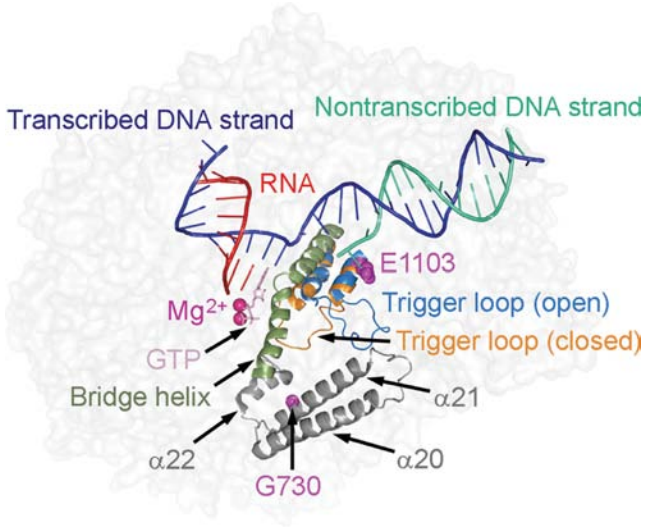

Figure 1. Locations of Rpb1 E1103 and G730 residues on the RNAP II structure. The RNAP II structures are based on PDB 2E2H (29), which has a closed trigger loop, and PDB 1Y1V (30), which has an open trigger loop, and generated by using PyMOL. Indicated structures are Rpb1 trigger loop (residues 1060–1105), bridge helix (residues 810–846) and α helices 20 (residues 673–699), 21 (residues 710–735) and 22 (residues 742–748), DNA, RNA, GTP and Mg^{2+}. Other residues of RNAP II are shown in transparent light gray.

We found that increased transcription bypass of CPDs by RNAP II enhances survival of UV-irradiated *S. cerevisiae* cells but attenuates TCR. The enhanced cell survival is independent of Rad26 or other NER factors. In contrast, impairment of transcription bypass of CPDs by RNAP II decreases survival of UV-irradiated GGR-deficient *S. cerevisiae* cells but enhances TCR. Our results suggest that transcription bypass of lesions may enhance lesion tolerance but attenuate TCR. Efficient stalling of RNAP II is essential for efficient TCR.

MATERIALS AND METHODS

Yeast strains and plasmids

All yeast strains used in this study are derivatives of the wild-type strain Y452 (*MATα*, *ura3–52*, *his3–1*, *leu2–3*, *leu2–112*, *cir°*). Deletions of *RAD16*, *RPB1*, *RAD26* and *RAD14* genes were conducted as previously described (23).

Plasmid pRS416-RPB1 was created by inserting the whole *RPB1* gene including the promoter, coding sequence and 3′ terminator sequences into the multiple cloning site of the centromeric *URA3* plasmid pRS416 (36). Plasmids pRS415-RPB1, pRS415-RPB1E1103G and pRS415-RPB1G730D were created by inserting the whole *RPB1* gene encoding the wild-type and E1103G and G730D mutant Rpb1, respectively, into the XhoI and ApaI sites of the centromeric *LEU2* plasmid pRS415 (36).

Plasmids pRS415-RPB1, pRS415-RPB1E1103G and pRS415-RPB1G730D were transformed into yeast strains

whose genomic *RPB1* gene was deleted and complemented with pRS416-RPB1. The transformed cells were selected with 5-fluoroorotic acid, which is toxic to cells with a functional *URA3* gene, to select for cells that had lost the pRS416-RPB1 plasmid.

Measurement of RNA synthesis in yeast cells

To measure total RNA synthesis, yeast cells were grown at 30°C in synthetic dextrose medium to late log phase (A_{600} ≈ 1.0). The harvested cells were washed twice with ice-cold H_2O, resuspended in ice-cold 2% dextrose and split into two aliquots. One aliquot was kept on ice and the other was irradiated with 360 J/m^2 of 254 nm UV (by using a 15W UV germicidal bulb, General Electric). Treatment of genomic DNA with T4 endonuclease V, followed by denaturing agarose gel analysis indicates that this dose of UV induces ∼1 CPD per 1 kb of DNA. After addition of one-tenth volume of a stock solution (6.7% yeast nitrogen base without amino acids, 1.6% yeast synthetic drop-out media supplement without uracil, 1 mM uracil), [2–^{14}C]uracil (56.0 mCi/mmol; Moravek Biochemicals) was added to a final concentration of 2 μM. The samples were incubated at 30°C in the dark and aliquots were collected at different times of the incubation. Total RNA was isolated using a hot acidic phenol method as previously described (37), and quantified by using the Qubit® RNA HS assay kit and a Qubit® 2.0 Fluorometer (Invitrogen, Life Technologies). The isolated total RNA was fractionated on formaldehyde agarose gels (38), and transferred onto Hybond-N$^+$ membranes (GE Healthcare Life Sciences). The membranes were exposed to Phosphorimager screens for 7 days and scanned with Molecular Imager FX (Bio-Rad).

For northern blot analysis of galactose-induced *GAL10* transcription, yeast cells were grown at 30°C in synthetic medium containing 2% glycerol, 2% lactate and 2% ethanol to late log phase (A_{600} ≈ 1.0). The harvested cells were washed and resuspended in ice-cold H_2O, and split into two aliquots. One aliquot was kept on ice and the other was irradiated with 120 J/m^2 of 254 nm UV (the dose we used for TCR analysis). The unirradiated and UV-irradiated cells were pelleted by centrifugation and resuspended in YPG (1% yeast extract, 2% peptone and 2% galactose) medium and incubated at 30°C. At different times of the incubation, aliquots were collected. Total RNA was isolated, fractionated on formaldehyde agarose gels and transferred onto Hybond-N$^+$ membranes. The *GAL10* transcripts on the membranes were probed with a 150 nucleotide long [α-^{32}P] UTP-labeled riboprobe that is complementary to the 5′ end of the *GAL10* transcripts.

Repair analysis of UV-induced CPDs

Yeast cells were cultured at 30°C in synthetic dextrose medium to late log phase (A_{600} ≈ 1.0), washed twice with ice-cold ddH_2O, resuspended in 2% dextrose and irradiated with 120 J/m^2 of 254 nm UV. After addition of one-tenth volume of a stock solution (10% yeast extract, 20% peptone), the yeast samples were incubated at 30°C in the dark. At different times of the repair incubation, aliquots were collected and the genomic DNA was isolated as described previously (23).

The transcribed and non-transcribed strands of the *RPB2* gene (39,40) were 3′-end labeled with [α-^{32}P]dATP by using a method described previously (41,42). Briefly, ∼1 μg of total genomic DNA was digested with DraI to release the *RPB2* fragments and incised at CPD sites with an excess amount of T4 endonuclease V (Epicentre). Excess copies of a biotinylated oligonucleotide, which is complementary to the 3′ end of the transcribed or non-transcribed strand of the *RPB2* gene, were mixed with the samples. The mixtures were heated at 95°C for 5 min to denature the DNA and then cooled to an annealing temperature of around 50°C. The annealed molecules were attached to streptavidin magnetic beads, labeled with [α-^{32}P]dATP and resolved on DNA sequencing gels. The gels were exposed to Phosphorimager screens. The intensities of gel bands corresponding to CPD sites were quantified using Quantity One (Bio-Rad).

UV sensitivity assay

Yeast cells were cultured at 30°C in synthetic dextrose medium to saturation. Sequential 10-fold dilutions of the cultures were made. For spotting assay, the diluted cells were spotted onto YPD (1% yeast extract, 2% peptone and 2% dextrose) plates and irradiated with different doses of 254 nm UV. After 3–5 days of incubation at 30°C in the dark, the plates were photographed. For colony formation assay, the diluted cells were spread onto YPD plates and irradiated with different doses of 254 nm UV. After 3–5 days of incubation at 30°C in the dark, the colonies were counted. Three repeats were performed and the means and standard deviations were calculated.

Detection of cellular levels of Rpb1 by western blot

Late log phase yeast cells were harvested and the whole cell extracts were prepared as described previously (43). Proteins were resolved on an sodium dodecyl sulphate-polyacrylamide gel electrophoresis (SDS-PAGE) gel and transferred onto a polyvinylidene difluoride membrane (Immobilon-P; Millipore). Rpb1 and glyceraldehyde-3-phosphate dehydrogenase, loading control (GAPDH), were probed with 8WG16 (Neoclone), which recognizes the C-terminal repeats of Rpb1, and GAPDH Loading Control Antibody (Thermol Scientific). Blots were incubated with SuperSignal West Femto Maximum Sensitivity Substrate (Thermo Scientific), and the protein bands were detected using ChemiDoc™ XRS+ System (Bio-Rad).

Measurement of RNAP II densities on the *RPB2* gene by chromatin immunoprecipitation (ChIP) assay

The ChIP assay was performed as described previously (44). Briefly, yeast cells were grown in synthetic dextrose medium to late log phase, cross-linked with 1% formaldehyde and lysed by vortexing with glass beads. The cell lysates were sonicated by using a Bioruptor (Diagenode) to shear the chromatin DNA to an average size of 200 bp and clarified by centrifugation at 4°C. An aliquot from each of the clarified lysates was saved as an input. The remaining lysates were immunoprecipited with the anti-Rpb1 antibody 8WG16 or

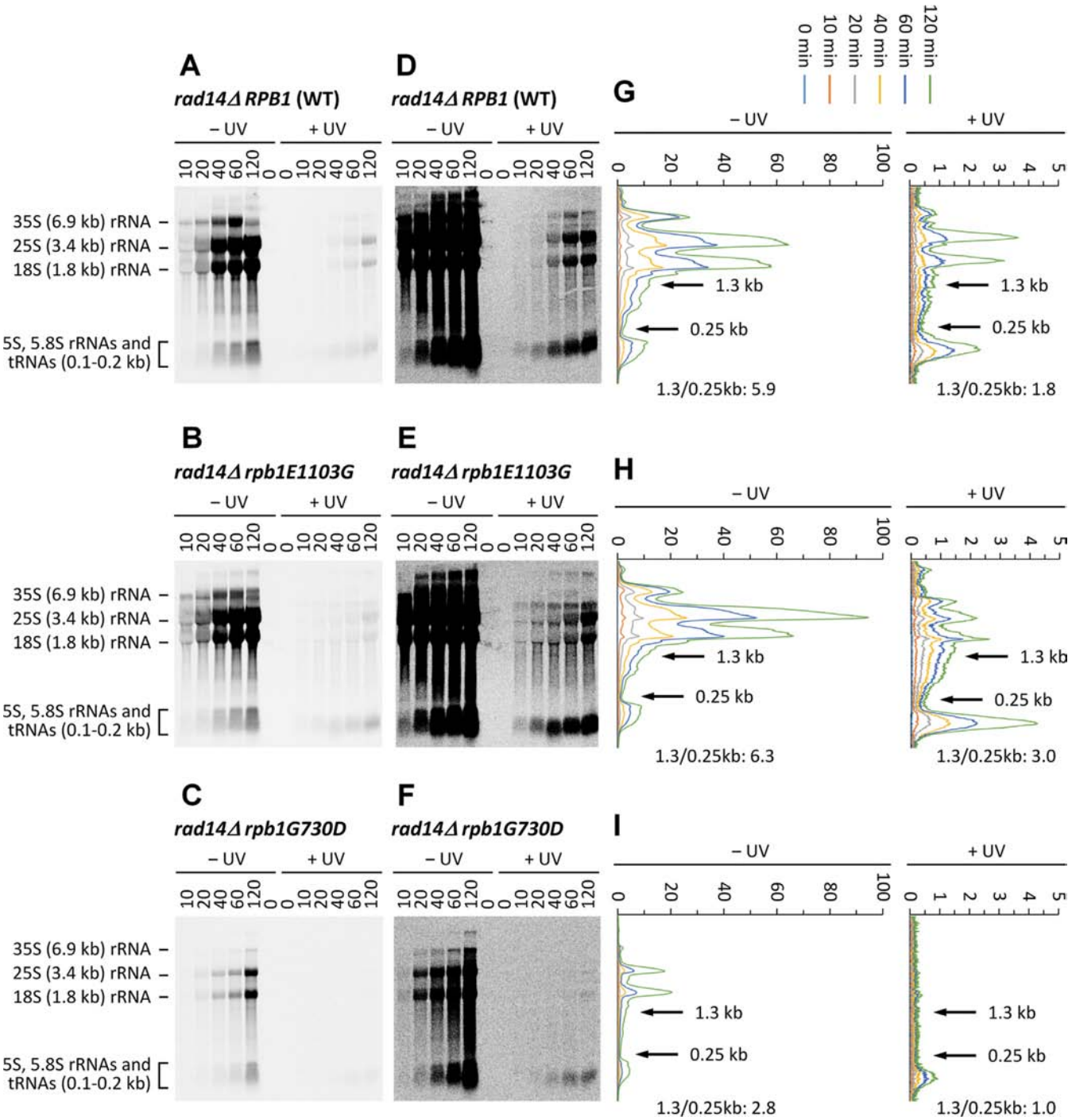

Figure 2. Effects of *rpb1E1103G* and *rpb1G730D* mutations on overall transcription *in vivo*. (A–C) Gel blots showing incorporation of ^{14}C uracil into different species of RNAs in UV-irradiated and unirradiated *rad14Δ* cells expressing wild-type Rpb1, and *rpb1E1103G* and *rpb1G730D* mutants. Numbers on the top of the blots indicate time (min) of incubation at 30°C. rRNA and tRNA species are marked on the left of the blots. mRNAs, most of which are in the size range of 0.3–5 kb (average 1.3 kb) (45), migrated as smear. (D–F) Same blots as those of A–C, respectively, but with higher exposure. (G–I) Plots showing scans of ^{14}C signal intensities along the lanes of the gel blots shown in A–C, respectively. Numbers on top of the plots indicate relative signal intensity (arbitrary units). The ratio of signal intensities between the transcripts of around 1.3 kb and those of around 0.25 kb after 120 min of incubation is shown at the bottom of each plot.

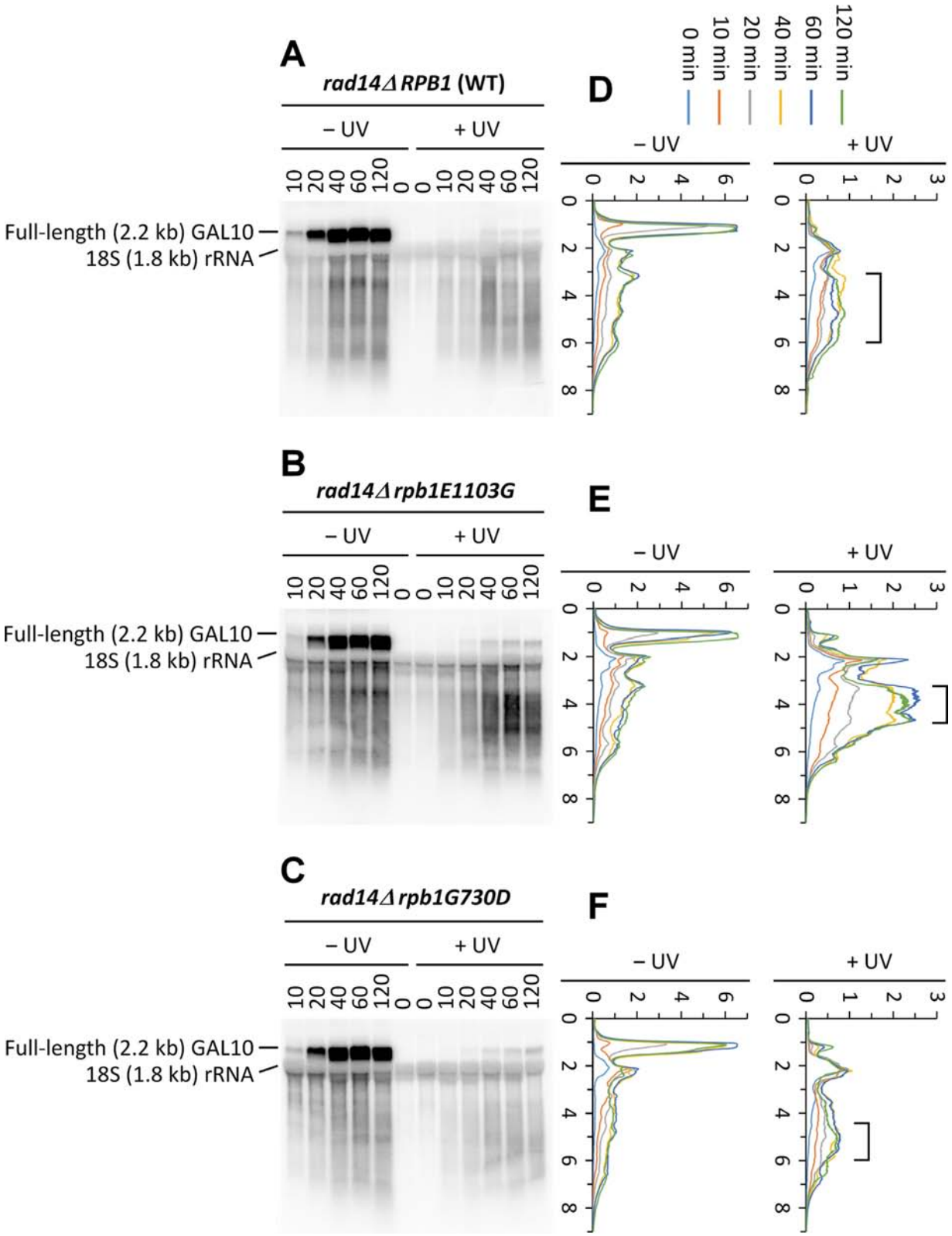

Figure 3. Effects of *rpb1E1103G* and *rpb1G730D* mutations on *GAL10* transcription. (A–C) Northern blots showing *GAL10* transcripts in UV-irradiated and unirradiated *rad14Δ* cells expressing wild-type Rpb1, and *rpb1E1103G* and *rpb1G730D* mutants. Note that the 18S rRNA has certain level of cross-hybridization with the *GAL10* riboprobe. Numbers on top of the blots indicate time (min) of incubation in galactose medium at 30°C. (D–F) Plots showing scans of signal intensities along the lanes of the blots shown in A–C, respectively. Numbers on the top of the plots indicate relative signal intensity (arbitrary units). Numbers on the left of the plots indicate relative locations on the gel (arbitrary units). Brackets on the right panels indicate the predominant *GAL10* transcripts.

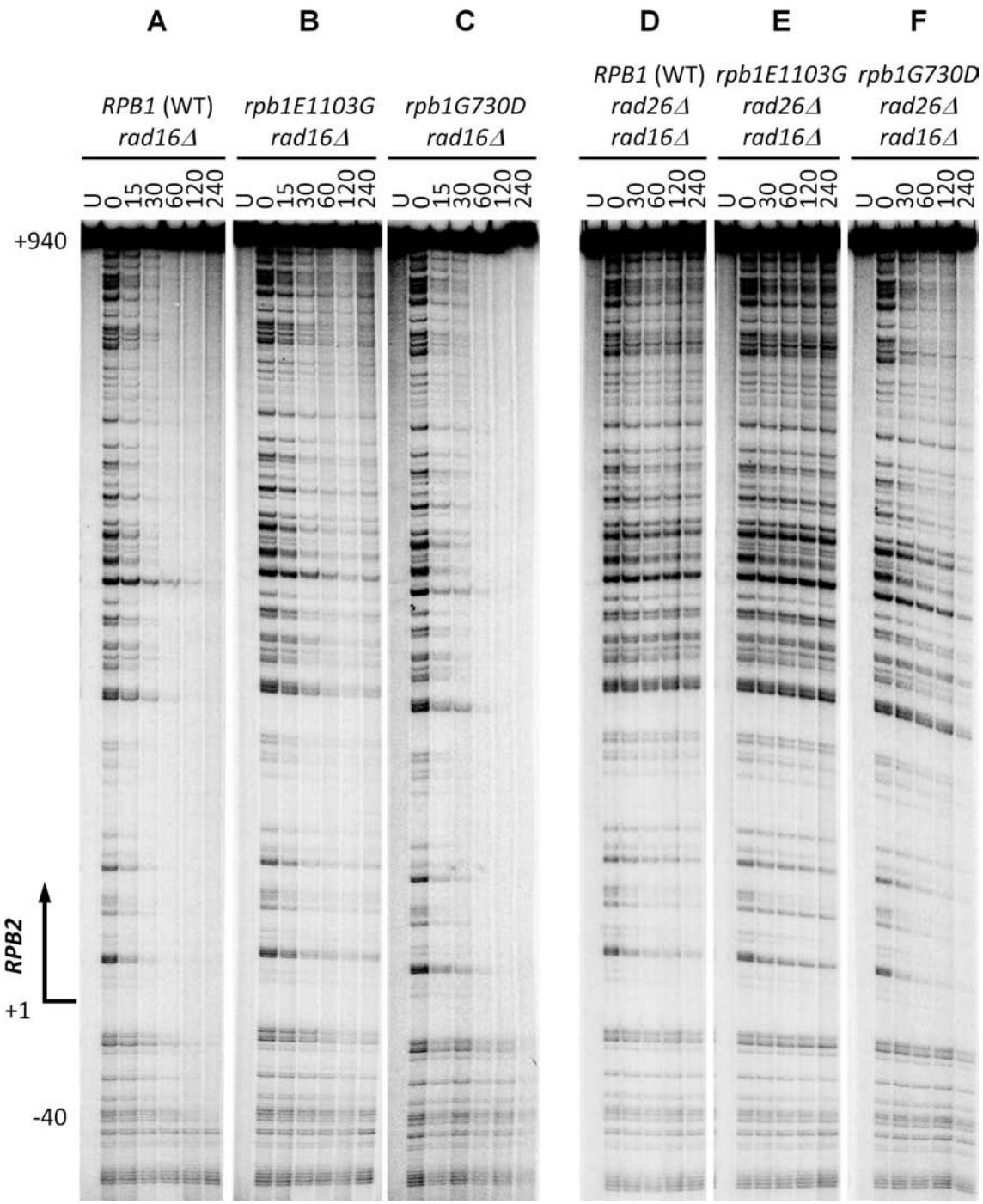

Figure 4. Effects of *rpb1E1103G* and *rpb1G730D* mutations on TCR. (A–C) Sequencing gel showing TCR of CPDs in *rad16Δ* cells expressing wild-type Rpb1, and *rpb1E1103G* and *rpb1G730D* mutants. (D–F) Sequencing gel showing TCR of CPDs in *rad16Δ rad26Δ* cells expressing wild-type Rpb1, and *rpb1E1103G* and *rpb1G730D* mutants. Unirradiated (U) and irradiated samples after different times (in minutes) of repair incubation are indicated at the top of the gel lanes. Nucleotide positions shown on the left are relative to the TSS.

mock immunoprecipitated. DNA fragments corresponding to different regions of the *RPB2* gene in the input, immunoprecipitated and mock immunoprecipitated samples were quantified in triplicates by using real-time polymerase chain reaction (PCR). Primers used for amplifying the different regions of the *RPB2* gene were described previously (20). The number of molecules in each immunoprecipitated sample was subtracted by that in the corresponding mock immunoprecipitated sample (generally ∼5% of the immunoprecipitated sample) and then normalized to that in the corresponding input. The levels of RNAP II association with the different regions of *RPB2* gene in cells expressing the *rpb1E1103G* and *rpb1G730D* mutants were normalized to

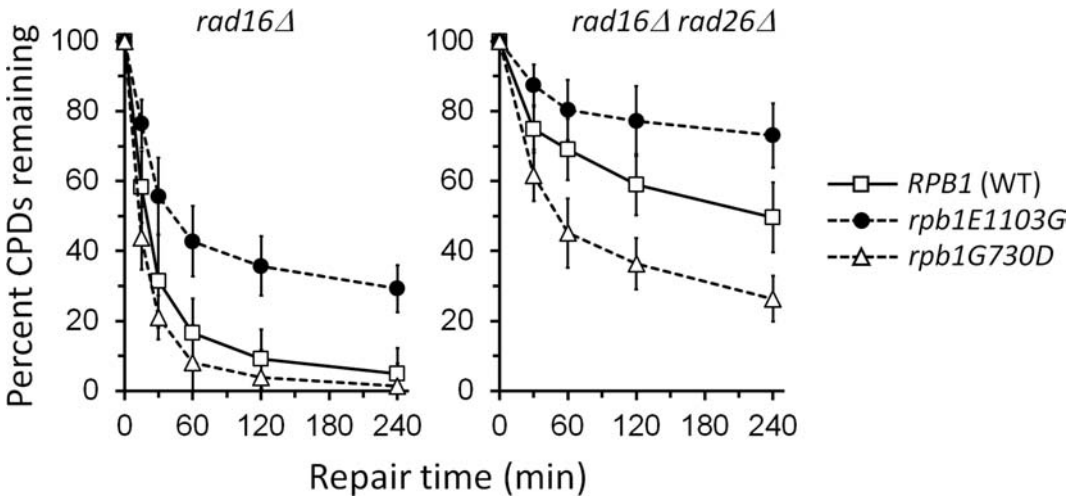

Figure 5. Percent of CPDs remaining in the transcribed strand of the *RPB2* gene in *rad16Δ* and *rad16Δ rad26Δ* cells expressing wild-type Rpb1, and *rpb1E1103G* and *rpb1G730D* mutants. Data are represented as mean ± SD.

those in cells expressing the wild-type Rpb1. The Student's *t*-test was used for statistical analysis.

RESULTS

rpb1E1103G mutation promotes transcription of UV-damaged templates, whereas *rpb1G730D* mutation impairs transcription of the damaged templates *in vivo*

In vitro studies with purified yeast RNAP II have shown that the *rpb1E1103G* mutation promotes transcription bypass of CPDs, whereas the *rpb1G730D* mutation abolishes transcription bypass of the DNA lesions (28). RNAP II transcription is affected by chromatin structure and regulated by a plethora of transcription elongation factors in the cell. To determine if the Rpb1 mutations also affect transcription bypass of lesions *in vivo*, we measured RNAP II transcription by detecting incorporation of radioactive ^{14}C uracil into total RNA in yeast cells. To prevent removal of UV-induced DNA lesions, we utilized *rad14Δ* cells, which are completely deficient in NER (2). Late log phase yeast cells were irradiated with 360 J/m^2 of 254 nm UV to induce ∼1 CPD per 1 kb of DNA. Unirradiated and the UV-irradiated cells were then incubated in the presence of ^{14}C uracil. Total RNA was isolated from the cells at different times of the incubation, fractionated on formaldehyde agarose gels and transferred onto membranes. The radioactive signals on the membranes were detected with a Phosphoimager.

The 35S (6.9 kb) unspliced rRNA precursor, which is transcribed by RNAP I, and the spliced 25S (3.4 kb) and 18S (1.8 kb) rRNAs migrated as distinct bands. Small (100–200 nucleotides long) RNA species, including tRNAs and 5S rRNA, which are transcribed by RNAP III, and the 5.8S rRNA, which is spliced from the 35S rRNA precursor, migrated as a diffused band at the bottom of the gels (Figure 2). mRNAs, which are transcribed by RNAP II and predominantly in the range of 0.3–5 kb (average 1.3 kb) (45), migrated as smears. ^{14}C uracil was rapidly incorporated into the different RNA species in the unirradiated *rad14Δ RPB1* (wild-type) and *rad14Δ rpb1E1103G* cells. The incorporation was slower in the unirradiated *rad14Δ rpb1G730D* cells, indicating that the mutation causes decreased transcription. The *rpb1G730D* cells grow very slowly, which is likely caused by decreased synthesis of mRNAs by RNAP II, which in turn results in decreased synthesis of other RNA species by other RNAPs.

UV irradiation greatly decreased incorporation of ^{14}C uracil into RNAs. However, the *rad14Δ rpb1E1103G* cells had a higher level of incorporation of ^{14}C uracil into mRNAs than *rad14Δ RPB1* cells, whereas the *rad14Δ rpb1G730D* cells showed very little level of the incorporation after UV irradiation (Figure 2G–I). To see how the different Rpb1 mutations affect transcription elongation of mRNAs, we calculated the ratios of signal intensities between transcripts of around 1.3 kb and those of around 0.25 kb. Transcripts of these lengths were well separated from the bands of the big rRNAs and small RNA species on the gel. A higher ratio will indicate that more shorter transcripts were elongated into longer transcripts, and thus reflect a more proficient transcription elongation. After 120 min of incubation, the ratios were 5.9 and 1.8 in unirradiated and UV-irradiated *rad14Δ RPB1* cells, respectively (Figure 2G), indicating UV-induced DNA lesions impaired transcription elongation of mRNAs. The ratios were 3.0 and 1.0 in UV-irradiated *rad14Δ rpb1E1103G* and *rad14Δ rpb1G730D* cells, respectively (Figure 2H and I). These results suggest that the *rpb1E1103G* and *rpb1G730D* mutations respectively promotes and impairs transcription elongation of mRNAs on UV-damaged templates. These results agree well with the *in vitro* observations that the Rpb1E1103G and G730D mutations respectively promotes and abolishes transcription bypass of DNA lesions (28).

To specifically analyze the effects of the *rpb1E1103G* and *rpb1G730D* mutations on RNAP II transcription and rule out the interference by transcripts of other RNAPs, we measured *GAL10* transcripts in UV-irradiated cells. The *GAL10* gene is not transcribed in glycerol/lactate/ethanol media, but can be rapidly induced upon switching of the cells to galactose media (46). Yeast cells were grown in a glycerol/lactate/ethanol medium to late log phase, irradiated with 120 J/m^2 of UV (the dose we used for TCR analy-

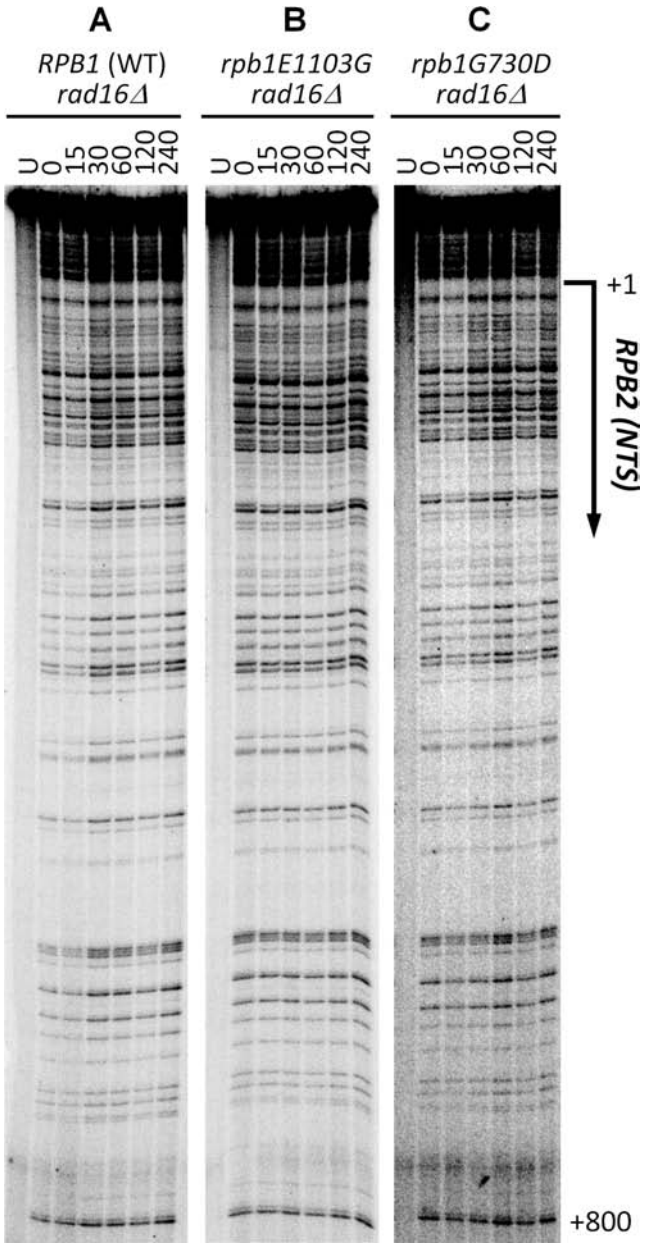

Figure 6. No repair of CPDs occurred in the non-transcribed strand of the *RPB2* gene in *rad16Δ* cells expressing wild-type Rpb1, and *rpb1E1103G* and *rpb1G730D* mutants.

ses) and switched to a galactose medium. For unknown reason(s), the *rpb1G730D* mutant cells grow almost as quickly as wild-type cells in glycerol/lactate/ethanol or galactose media (not shown). Total RNA was isolated from the cells at different times of incubation in the galactose medium. The *GAL10* transcripts were detected on northern blots by using a riboprobe that is complementary to the 5′ end of the *GAL10* transcripts.

GAL10 transcripts could be easily detected in all the yeast cells analyzed after 10 min of galactose induction and leveled off after ∼40 min of the induction (Figure 3). UV irradiation impaired the transcription of *GAL10* gene. The *rad14Δ rpb1E1103G* cells had a higher level of the *GAL10* transcripts than *rad14Δ RPB1* cells, whereas the *rad14Δ rpb1G730D* cells showed a lower level of the transcripts. Also, the predominant *GAL10* transcripts were longest in the *rad14Δ rpb1E1103G* cells and shortest in the *rad14Δ rpb1G730D* cells (Figure 3D and E). A higher level of longer transcripts will indicate more proficient transcription elongation, and *vice versa*. Taken together, our results indicate that the *rpb1E1103G* and *rpb1G730D* mutations respectively promotes and impairs transcription elongation of the UV-damaged *GAL10* gene. However, full-length *GAL10* transcripts were rare in all the cells analyzed, indicating that even the *rpb1E1103G* mutation may not enable full transcription bypass of UV lesions.

rpb1E1103G mutation attenuates TCR, whereas *rpb1G730D* mutation enhances TCR

To determine the implication of transcription bypass of DNA lesions in TCR, we directly measured repair of UV-induced CPDs in the *RPB2* gene in *rad16Δ RPB1*, *rad16Δ rpb1E1103G* and *rad16Δ rpb1G730D* yeast cells. The reason for using *rad16Δ* cells for the measurement is to eliminate GGR so that TCR can be unambiguously analyzed. Indeed, repair could not be seen in the region of the transcribed strand that is 40 nucleotides upstream of the transcription start site (TSS) (where TCR does not operate) (Figure 4A–F), or in the non-transcribed strand of the *RPB2* gene (Figure 6A–C). TCR could be easily seen in *rad16Δ RPB1* cells (Figure 4A). As expected, additional deletion of *RAD26* decreased TCR (Figure 4D). Surprisingly, the *rpb1E1103G* mutation caused attenuation of TCR in both *rad16Δ* and *rad16Δ rad26Δ* cells (Figure 4, compare panels A and B, and D and E; Figure 5). In contrast, the *rpb1G730D* mutation enhanced TCR in both *rad16Δ* and *rad16Δ rad26Δ* cells (Figure 4, compare panels A and C, and D and F; Figure 5).

Our results indicate that enhanced transcription bypass of DNA lesions attenuates TCR regardless the presence of Rad26. On the other hand, impaired transcription bypass of DNA lesions enhances Rad26-dependent and independent TCR.

rpb1E1103G mutation increases cell resistance to UV regardless the presence of any NER subpathways, whereas *rpb1G730D* mutation decreases cell resistance to UV only in the absence of GGR

The *rpb1E1103G* mutation was observed to increase UV resistance of *RAD26* cells but not that of *rad26Δ* cells, suggesting that the increased resistance is dependent on Rad26-dependent TCR (28). Our direct analysis of TCR showed that the mutation actually attenuate TCR regardless of the presence of Rad26. To determine if the increased UV resistance is dependent on Rad26-dependent TCR or other subpathway of NER, we measured epistatic interactions of the *rpb1E1103G* and *rpb1G730D* mutations with *RAD26*, which plays an important role in TCR, and with *RAD16* and *RAD14*, which are essential for GGR and the entire NER, respectively. The *rpb1E1103G* mutation increases UV resistance of the otherwise wild-type, *rad26Δ* (Figure 7A), *rad16Δ*, *rad16Δ rad26Δ* (Figure 7B and D) and *rad14Δ*

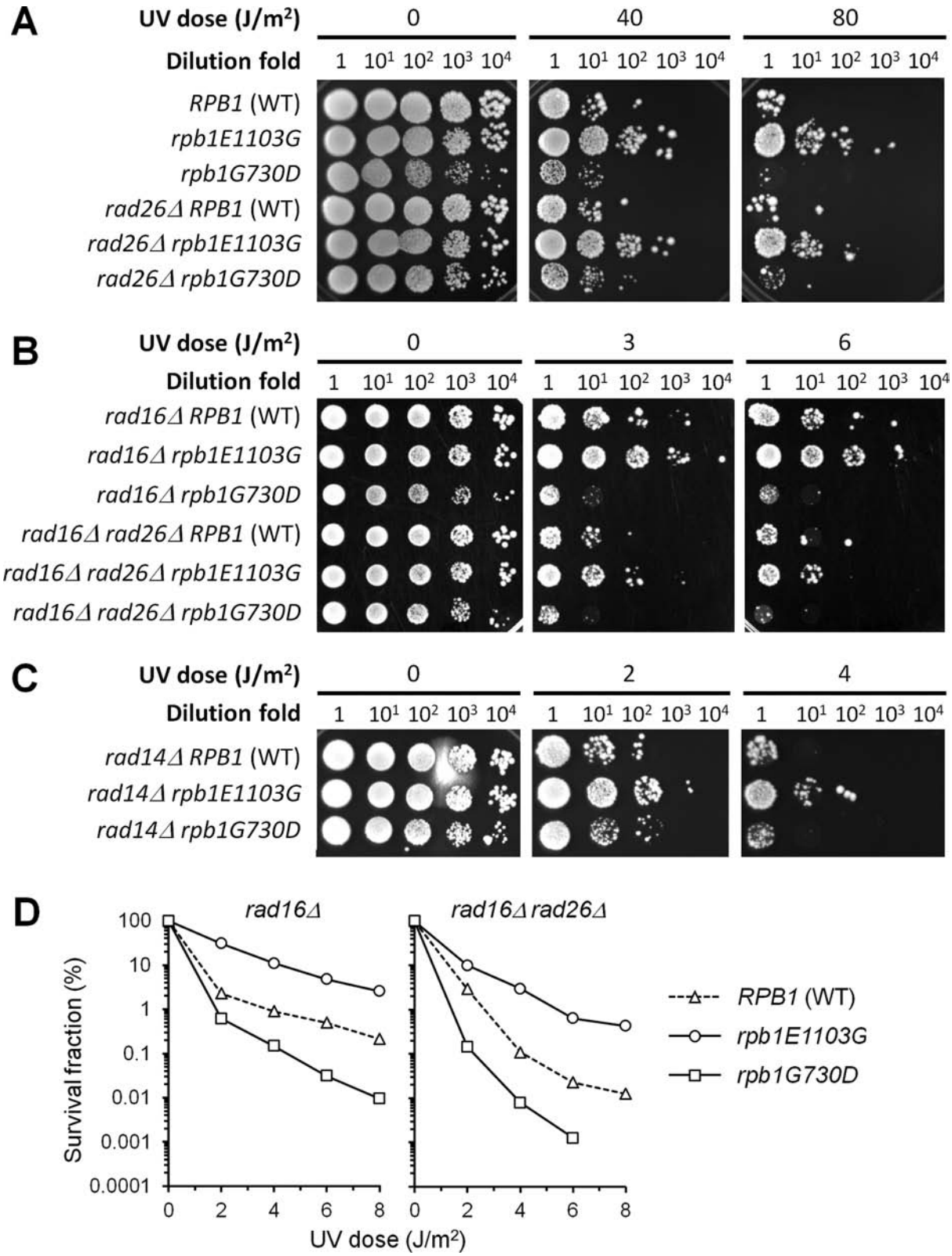

Figure 7. Epistatic interactions of *rpb1E1103G* and *rpb1G730D* mutations with different NER genes. (A–C) Spotting assay showing the effects of *rpb1E1103G* and *rpb1G730D* mutations on UV sensitivities of yeast cells with different NER subpathways operative. (D) Colony formation assay showing the effects of *rpb1E1103G* and *rpb1G730D* mutations on UV sensitivities of *rad16Δ* and *rad16Δ rad26Δ* cells. The values of the survival fractions are the means of three repeats. Standard error bars are within the symbols of the data points.

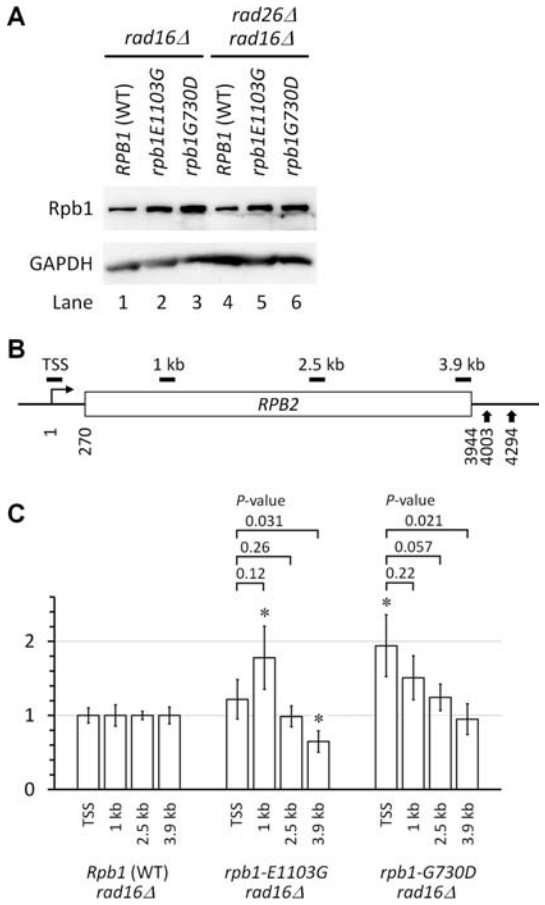

Figure 8. Both *rpb1E1103G* and *rpb1G730D* mutations cause a deficiency in transcription processivity. (A) Western blot showing expression levels of the wild-type Rpb1 and *rpb1E1103G* and *rpb1G730D* mutants in *rad16Δ* and *rad16Δ rad26Δ* cells. The GAPDH is used as loading control. (B) Schematic of the *RPB2* gene. Nucleotide positions are relative to the TSS. Vertical arrows at the 3′ end of the gene indicate the two alternative polyadenylation sites (39). Short horizontal bars above the schematic indicate regions of 134–150 bp amplified by real-time PCR for quantification of ChIP fragments of the *RPB2* gene (20). (C) RNAP II densities in different regions of the *RPB2* gene. The RNAP II densities in the TSS, 1, 2.5 and 3.9 kb regions of the *RPB2* gene in *RPB1* (wild-type) cells were normalized to 1. The densities of *rpb1E1103G* and *rpb1G730D* mutant RNAP II in the different regions of the *RPB2* gene are relative to those in the corresponding regions of the *RPB2* gene in *RPB1* cells. The values of RNAP II densities are represented as mean (±SD) of three ChIP experiments. Single asterisks (*) denote a *P*-value of <0.05, in the Student's *t*-test between the mutant and wild-type cells for RNAP II densities in the corresponding regions of the *RPB2* gene. Above the bars of *rpb1E1103G* and *rpb1G730D* samples are shown the *P*-values of Student's *t*-test between the TSS region and the 1, 2.5 or 3.9 kb region (a *P*-value of <0.05 is considered to be significant).

(Figure 7C) cells. These results indicate that the increased UV resistance is independent of Rad26-dependent TCR, GGR or the entire NER. Rather, the increased UV resistance is likely due to enhanced lesion tolerance conferred by increased transcription bypass of the lesions. Our results do not agree with the previous report showing that the increased UV resistance of the *rpb1E1103G* mutants is dependent on Rad26 (28). The reason for the discrepancy is unknown, but may be caused by strain background differences. All the strains used in this study were created in the Y452 background.

The *rpb1G730D* mutation decreases UV resistance of *rad16Δ* and *rad16Δ rad26Δ* cells (Figure 7B and D), but has no effect on UV resistance of wild-type, *rad26Δ* (Figure 7A) and *rad14Δ* (Figure 7C) cells. These results suggest that, in the absence of Rad16-mediated GGR, abolition of transcription bypass of lesions decreases DNA lesion tolerance, although the abolition enhances TCR.

The decreased UV resistance of the *rpb1G730D* mutant may be caused not only by stalling at DNA lesions but also by lower overall transcription processivity, which may lead to aberrant transcription of multiple genes and, as a result, destabilizes cellular metabolism in general. We therefore examined the expression levels of the wild-type Rpb1 and the *rpb1G730D* and *rpb1E1103G* mutants, and measured the densities of RNAP II in different regions of the *RPB2* gene. The *rpb1E1103G* and *rpb1G730D* mutant proteins were expressed to similar levels that were approximately twice as high as the wild-type Rpb1 (Figure 8A). The density of the *rpb1E1103G* mutant RNAP II in the 1-kb region of the *RPB2* gene was higher than that of the wild-type RNAP II, indicating that this mutant RNAP II tends to pause at this region (Figure 8B and C). The density of the *rpb1G730D* mutant RNAP II was higher than that of the wild-type RNAP II in the region around TSS of the *RPB2* gene. The higher expression levels of the Rpb1 mutants may enable more efficient loading of the mutant RNAP II to the promoter, leading to high densities toward the 5′ end of the *RPB2* gene. The densities of *rpb1E1103G* and *rpbG730D* mutant RNAP II decreased toward the 3′ end of the *RPB2* gene (Figure 8C), indicating that both mutants have a deficiency in transcription processivity. Therefore, the decreased UV resistance of the *rpb1G730D* mutant may not be primarily caused by a lower overall transcription processivity, as the *rpb1E1103G* mutant has similar deficiency in transcription processivity but shows increased UV resistance.

DISCUSSION

We showed here that increased transcription bypass of CPDs attenuates TCR but enhances cell survival, whereas impairment of the bypass enhances TCR but decreases cell survival in the absence of GGR. Our results do not support the proposition that the bypass, which may expose the lesions, is required for TCR (28,35). Rather, the bypass may actually weaken the recognition of lesions during TCR.

Transcription bypass of a DNA lesion could have serious repercussions on the cell, particularly if the lesion has miscoding properties, resulting in the insertion of incorrect nucleotides into the mRNA and generation of a mutant protein (25). However, the bypass may allow the completion of the ongoing mRNA synthesis to provide a steady supply of the housekeeping and repair proteins in the presence of the lesions, thereby enhancing cell survival. Therefore, the bypass may serve as a DNA damage tolerance mechanism that is alternative to TCR. The survival benefit of the damage tolerance appears to outweigh the survival deficiency of TCR attenuation caused by enhanced transcription bypass of DNA lesions.

Our results offer direct evidence for the long-standing but unproven notion that TCR requires sufficient stalling of an RNAP. Incorporation of one or two nucleotides opposite a CPD, especially misincorporation of a nucleotide opposite the 5′ nucleotide of a CPD appears to be necessary to induce RNAP II stalling and potentially invoke TCR (28,47–48). We show here that the *rpb1G730D* mutation, which blocks RNAP II by preventing nucleotide incorporation opposite both the 3′ and 5′ nucleotides of a CPD, enhances TCR. This suggests that sufficient stalling of RNAP II, regardless of incorporation or misincorporation of nucleotides opposite a lesion, may be sufficient for eliciting TCR. However, transcription is regulated by a plethora of transcription elongation factors in the cell, if the *rpb1G730D* mutant RNAP II can catalyze incorporation of nucleotides across CPDs that leads to transcription stalling *in vivo* has not been tested. Therefore, if the enhanced TCR caused by the *rpb1G730D* mutation requires the incorporation or misincorporation of nucleotide(s) across CPDs in living yeast cells remains to be determined. Besides enhancing TCR, stalling of RNAP II blocks ongoing transcription and may also impair replication, resulting in reduced resistance to DNA damage especially in the absence of GGR. In this case, the survival deficiency caused by impaired transcription bypass of DNA lesions outweighs the survival benefit of enhanced TCR.

Previous studies have ruled out the roles of ubiquitination and degradation of Rpb1 (49–51) and back-tracking of RNAP II by TFIIS (52) in TCR. A number of transcription elongation factors, such as Spt4 (22), Spt5 (20,21) and PAFc (24), which stabilize and promote forward-tracking of the RNAP II elongation complex, have been shown to repress TCR. Here, we show that transcription bypass of lesions attenuates TCR, although the bypass may expose the lesions to DNA repair machinery. Taken together, these studies appear to support the model that the RNAP II complex stalled at a lesion may be remodeled, rather than removed from the stalled site, to initiate TCR in eukaryotic cells. How RNAP II complex is remodeled during TCR remains to be elucidated.

ACKNOWLEDGEMENT

We thank our laboratory members for inspiring discussion.

FUNDING

National Science Foundation [MCB-1244019 to SL]. Funding for open access charge: National Science Foundation [MCB-1244019 to SL].
Conflict of interest statement. None declared.

REFERENCES

1. Scharer,O.D. (2013) Nucleotide excision repair in eukaryotes. *Cold Spring Harb Perspect. Biol.*, **5**, a012609.
2. Tatum,D. and Li,S. (2011) In: Storici,F (ed). *DNA Repair - On the Pathways to Fixing DNA Damage and Errors*. InTech Open Access Publisher, Rijeka, Croatia, pp. 97–122.
3. Sarasin,A. (2012) UVSSA and USP7: new players regulating transcription-coupled nucleotide excision repair in human cells. *Genome Med.*, **4**, 44.
4. Schwertman,P., Vermeulen,W. and Marteijn,J.A. (2013) UVSSA and USP7, a new couple in transcription-coupled DNA repair. *Chromosoma*, **122**, 275–284.
5. Lindsey-Boltz,L.A. and Sancar,A. (2007) RNA polymerase: the most specific damage recognition protein in cellular responses to DNA damage? *Proc. Natl. Acad. Sci. U.S.A.*, **104**, 13213–13214.
6. Selby,C.P., Drapkin,R., Reinberg,D. and Sancar,A. (1997) RNA polymerase II stalled at a thymine dimer: footprint and effect on excision repair. *Nucleic Acids Res.*, **25**, 787–793.
7. Hanawalt,P.C. and Spivak,G. (2008) Transcription-coupled DNA repair: two decades of progress and surprises. *Nat. Rev. Mol. Cell Biol.*, **9**, 958–970.
8. Vermeulen,W. and Fousteri,M. (2013) Mammalian transcription-coupled excision repair. *Cold Spring Harb. Perspect. Biol.*, **5**, a012625.
9. Deaconescu,A.M., Chambers,A.L., Smith,A.J., Nickels,B.E., Hochschild,A., Savery,N.J. and Darst,S.A. (2006) Structural basis for bacterial transcription-coupled DNA repair. *Cell*, **124**, 507–520.
10. Howan,K., Smith,A.J., Westblade,L.F., Joly,N., Grange,W., Zorman,S., Darst,S.A., Savery,N.J. and Strick,T.R. (2012) Initiation of transcription-coupled repair characterized at single-molecule resolution. *Nature*, **490**, 431–434.
11. Park,J.S., Marr,M.T. and Roberts,J.W. (2002) E. coli Transcription repair coupling factor (Mfd protein) rescues arrested complexes by promoting forward translocation. *Cell*, **109**, 757–767.
12. Selby,C.P. and Sancar,A. (1993) Molecular mechanism of transcription-repair coupling. *Science*, **260**, 53–58.
13. Selby,C.P. and Sancar,A. (1995) Structure and function of transcription-repair coupling factor. I. Structural domains and binding properties. *J. Biol. Chem.*, **270**, 4882–4889.
14. Selby,C.P. and Sancar,A. (1995) Structure and function of transcription-repair coupling factor. II. Catalytic properties. *J. Biol. Chem.*, **270**, 4890–4895.
15. Haines,N.M., Kim,Y.I., Smith,A.J. and Savery,N.J. (2014) Stalled transcription complexes promote DNA repair at a distance. *Proc. Natl. Acad. Sci. U.S.A.*, **111**, 4037–4042.
16. Epshtein,V., Kamarthapu,V., McGary,K., Svetlov,V., Ueberheide,B., Proshkin,S., Mironov,A. and Nudler,E. (2014) UvrD facilitates DNA repair by pulling RNA polymerase backwards. *Nature*, **505**, 372–377.
17. Selby,C.P. and Sancar,A. (1997) Human transcription-repair coupling factor CSB/ERCC6 is a DNA-stimulated ATPase but is not a helicase and does not disrupt the ternary transcription complex of stalled RNA polymerase II. *J. Biol. Chem.*, **272**, 1885–1890.
18. van Gool,A.J., Citterio,E., Rademakers,S., van Os,R., Vermeulen,W., Constantinou,A., Egly,J.M., Bootsma,D. and Hoeijmakers,J.H. (1997) The Cockayne syndrome B protein, involved in transcription-coupled DNA repair, resides in an RNA polymerase II-containing complex. *EMBO J.*, **16**, 5955–5965.
19. Selby,C.P. and Sancar,A. (1997) Cockayne syndrome group B protein enhances elongation by RNA polymerase II. *Proc. Natl. Acad. Sci. U.S.A.*, **94**, 11205–11209.
20. Li,W., Giles,C. and Li,S. (2014) Insights into how Spt5 functions in transcription elongation and repressing transcription coupled DNA repair. *Nucleic Acids Res.*, **42**, 7069–7083.
21. Ding,B., LeJeune,D. and Li,S. (2010) The C-terminal repeat domain of Spt5 plays an important role in suppression of Rad26-independent transcription coupled repair. *J. Biol. Chem.*, **285**, 5317–5326.
22. Jansen,L.E., den Dulk,H., Brouns,R.M., de Ruijter,M., Brandsma,J.A. and Brouwer,J. (2000) Spt4 modulates Rad26 requirement in transcription-coupled nucleotide excision repair. *EMBO J.*, **19**, 6498–6507.
23. Li,S. and Smerdon,M.J. (2002) Rpb4 and Rpb9 mediate subpathways of transcription-coupled DNA repair in Saccharomyces cerevisiae. *EMBO J.*, **21**, 5921–5929.
24. Tatum,D., Li,W., Placer,M. and Li,S. (2011) Diverse roles of RNA polymerase II-associated factor 1 complex in different subpathways of nucleotide excision repair. *J. Biol. Chem.*, **286**, 30304–30313.
25. Saxowsky,T.T. and Doetsch,P.W. (2006) RNA polymerase encounters with DNA damage: transcription-coupled repair or transcriptional mutagenesis? *Chem. Rev.*, **106**, 474–488.
26. Xu,L., Da,L., Plouffe,S.W., Chong,J., Kool,E. and Wang,D. (2014) Molecular basis of transcriptional fidelity and DNA lesion-induced transcriptional mutagenesis. *DNA Repair*, **19**, 71–83.

27. Brueckner,F., Hennecke,U., Carell,T. and Cramer,P. (2007) CPD damage recognition by transcribing RNA polymerase II. *Science*, **315**, 859–862.
28. Walmacq,C., Cheung,A.C., Kireeva,M.L., Lubkowska,L., Ye,C., Gotte,D., Strathern,J.N., Carell,T., Cramer,P. and Kashlev,M. (2012) Mechanism of translesion transcription by RNA polymerase II and its role in cellular resistance to DNA damage. *Mol. Cell*, **46**, 18–29.
29. Wang,D., Bushnell,D.A., Westover,K.D., Kaplan,C.D. and Kornberg,R.D. (2006) Structural basis of transcription: role of the trigger loop in substrate specificity and catalysis. *Cell*, **127**, 941–954.
30. Kettenberger,H., Armache,K.J. and Cramer,P. (2004) Complete RNA polymerase II elongation complex structure and its interactions with NTP and TFIIS. *Mol. Cell*, **16**, 955–965.
31. Kireeva,M.L., Nedialkov,Y.A., Cremona,G.H., Purtov,Y.A., Lubkowska,L., Malagon,F., Burton,Z.F., Strathern,J.N. and Kashlev,M. (2008) Transient reversal of RNA polymerase II active site closing controls fidelity of transcription elongation. *Mol. Cell*, **30**, 557–566.
32. Koyama,H., Ueda,T., Ito,T. and Sekimizu,K. (2010) Novel RNA polymerase II mutation suppresses transcriptional fidelity and oxidative stress sensitivity in rpb9Delta yeast. *Genes Cells*, **15**, 151–159.
33. Malagon,F., Kireeva,M.L., Shafer,B.K., Lubkowska,L., Kashlev,M. and Strathern,J.N. (2006) Mutations in the Saccharomyces cerevisiae RPB1 gene conferring hypersensitivity to 6-azauracil. *Genetics*, **172**, 2201–2209.
34. Strathern,J., Malagon,F., Irvin,J., Gotte,D., Shafer,B., Kireeva,M., Lubkowska,L., Jin,D.J. and Kashlev,M. (2013) The fidelity of transcription: RPB1 (RPO21) mutations that increase transcriptional slippage in S. cerevisiae. *J. Biol. Chem.*, **288**, 2689–2699.
35. Ellenberger,T. (2012) An arresting development in transcription. *Mol. Cell*, **46**, 3–4.
36. Sikorski,R.S. and Hieter,P. (1989) A system of shuttle vectors and yeast host strains designed for efficient manipulation of DNA in Saccharomyces cerevisiae. *Genetics*, **122**, 19–27.
37. Collart,M.A. and Oliviero,S. (2004) In: Ausubel,FM, Brent,R, Kingston,RE, Moore,DD, Seidman,JG, Smith,JA and Struhl,K (eds). *Current Protocols in Molecular Biology*. John Wiley & Sons, Inc., New York, **2**, pp. 13.12.11–13.12.15.
38. Sambrook,J. and Russell,D.W. (2001) *Molecular Cloning: A Laboratory Manual*. Cold Spring Harbor Laboratory Press, Cold Spring Harbor, NY.
39. Yu,L. and Volkert,M.R. (2013) UV damage regulates alternative polyadenylation of the RPB2 gene in yeast. *Nucleic Acids Res.*, **41**, 3104–3114.
40. Sweetser,D., Nonet,M. and Young,R.A. (1987) Prokaryotic and eukaryotic RNA polymerases have homologous core subunits. *Proc. Natl. Acad. Sci. U.S.A.*, **84**, 1192–1196.
41. Li,S. and Waters,R. (1996) Nucleotide level detection of cyclobutane pyrimidine dimers using oligonucleotides and magnetic beads to facilitate labelling of DNA fragments incised at the dimers and chemical sequencing reference ladders. *Carcinogenesis*, **17**, 1549–1552.
42. Li,S., Waters,R. and Smerdon,M.J. (2000) Low- and high-resolution mapping of DNA damage at specific sites. *Methods*, **22**, 170–179.
43. Kushnirov,V.V. (2000) Rapid and reliable protein extraction from yeast. *Yeast*, **16**, 857–860.
44. Li,S., Chen,X., Ruggiero,C., Ding,B. and Smerdon,M.J. (2006) Modulation of Rad26- and Rpb9-mediated DNA repair by different promoter elements. *J. Biol. Chem.*, **281**, 36643–36651.
45. Hurowitz,E.H. and Brown,P.O. (2003) Genome-wide analysis of mRNA lengths in Saccharomyces cerevisiae. *Genome Biol.*, **5**, R2.
46. Lohr,D., Venkov,P. and Zlatanova,J. (1995) Transcriptional regulation in the yeast GAL gene family: a complex genetic network. *FASEB J.*, **9**, 777–787.
47. Brueckner,F. and Cramer,P. (2007) DNA photodamage recognition by RNA polymerase II. *FEBS Lett.*, **581**, 2757–2760.
48. Mei Kwei,J.S., Kuraoka,I., Horibata,K., Ubukata,M., Kobatake,E., Iwai,S., Handa,H. and Tanaka,K. (2004) Blockage of RNA polymerase II at a cyclobutane pyrimidine dimer and 6–4 photoproduct. *Biochem. Biophys. Res. Commun.*, **320**, 1133–1138.
49. Chen,X., Ruggiero,C. and Li,S. (2007) Yeast Rpb9 plays an important role in ubiquitylation and degradation of Rpb1 in response to UV-induced DNA damage. *Mol. Cell. Biol.*, **27**, 4617–4625.
50. Lommel,L., Bucheli,M.E. and Sweder,K.S. (2000) Transcription-coupled repair in yeast is independent from ubiquitylation of RNA pol II: implications for Cockayne's syndrome. *Proc. Natl. Acad. Sci. U.S.A.*, **97**, 9088–9092.
51. Woudstra,E.C., Gilbert,C., Fellows,J., Jansen,L., Brouwer,J., Erdjument-Bromage,H., Tempst,P. and Svejstrup,J.Q. (2002) A Rad26-Def1 complex coordinates repair and RNA pol II proteolysis in response to DNA damage. *Nature*, **415**, 929–933.
52. Verhage,R.A., Heyn,J., van de Putte,P. and Brouwer,J. (1997) Transcription elongation factor S-II is not required for transcription-coupled repair in yeast. *Mol. Gen. Genet.*, **254**, 284–290.